# An Arginine to Lysine Mutation in the Vicinity of the Heme Propionates Affects the Redox Potentials of the Hemes and Associated Electron and Proton Transfer in Cytochrome *c* Oxidase†

Denise A. Mills,‡ Lois Geren,§ Carrie Hiser,‡ Bryan Schmidt,‡,|| Bill Durham,§ Francis Millett,*,§ and Shelagh Ferguson-Miller*,‡

*Biochemistry and Molecular Biology Department, Michigan State University, East Lansing, Michigan 48824, and Department of Chemistry, University of Arkansas, Fayetteville, Arkansas 72701*

*Received February 16, 2005; Revised Manuscript Received June 8, 2005*

ABSTRACT: Cytochrome *c* oxidase pumps protons across a membrane using energy from electron transfer and reduction of oxygen to water. It is postulated that an element of the energy transduction mechanism is the movement of protons to the vicinity of the hemes upon reduction, to favor charge neutrality. Possible sites on which protons could reside, in addition to the conserved carboxylate E286, are the propionate groups of heme *a* and/or heme $a_3$. A highly conserved pair of arginines (R481 and R482) interact with these propionates through ionic and hydrogen bonds. This study shows that the conservative mutant, R481K, although as fully active as the wild type under many conditions, exhibits a significant decrease in the midpoint redox potential of heme *a* relative to $Cu_A$ ($\Delta E_m$) of $\cong$40 mV, has lowered activity under conditions of high pH or in the presence of a membrane potential, and has a slowed heme $a_3$ reduction with dithionite. Another mutant, D132A, which strongly inhibits proton uptake from the internal side of the membrane, has <4% of the activity of the wild type and appears to be dependent on proton uptake from the outside. A double mutation, D132A/R481K, is even more strongly inhibited ($\sim$1% of that of the wild type). The more-than-additive effect supports the concept that R481K not only lowers the midpoint potential of heme *a* but also limits a supply route for protons from the outside of the membrane used by the D132 mutant. The results are consistent with an important role of R481 and heme $a/a_3$ propionates in proton movement in a reversible exit path.

Cytochrome *c* oxidase (C*c*O)[1] is an integral membrane protein and is the terminal electron acceptor in the respiratory chain. Electrons from cytochrome *c* enter C*c*O through a dinuclear copper site ($Cu_A$) and move to heme *a*, heme $a_3$, and the closely associated $Cu_B$. Oxygen binding and reduction occur at the heme $a_3-Cu_B$ site (*1*). The electron transfer events and the chemical conversion of oxygen to water create a membrane potential by virtue of drawing protons from the inside and electrons from the outside of the membrane. In addition, C*c*O pumps protons through the protein to further build up the proton gradient $\Delta\mu H^+$ across the membrane. This gradient is then used to make ATP as a source of energy for the cell. The question of how the steps of electron transfer and the oxygen chemistry are coupled to the mechanism of proton pumping remains.

Intake paths for protons have been defined from the crystal structures (*2*−*5*) and by site-directed mutagenesis studies (*6*−*10*). A pathway discerned in bovine oxidase, the H path (*11*−*13*), has not been confirmed in prokaryotic C*c*O by mutagenesis studies (*14*), but two other paths, the D and K paths, appear to be highly conserved across a range of oxidases, including the mammalian C*c*O. The K path has a highly conserved lysine (K362) that is essential for reduction of the heme $a_3-Cu_B$ center (*10*, *15*−*17*) and appears to lead to the active site. The D path, so-called because of an important aspartate (D132) at the entrance, appears to end at a glutamate (E286) that is $\sim$12 Å from both hemes at their lower edges (Figure 1). Substitution of D132 for anything other than a carboxyl group inhibits proton uptake from the inside of the membrane, and net proton pumping is not observed. In fact, there is alkalinization on the outside of the D132A cytochrome *c* oxidase vesicles (COVs) during turnover, observed with the pH-sensitive dye phenol red (*18*).

D132A COVs exhibit the highest rates of oxygen consumption in the presence of a membrane potential (controlled state), a phenomenon that can be explained by backflow of protons from the outside, partially replacing the lack of

† Supported by National Institutes of Health Grants GM 26916, GM 57323, and GM 25480 (to S.F.-M.), and GM 20488 (to F.M., L.G., and B.D.) and NCRR COBRE 1 P20 RR15569 (F.M. and B.D.).

* To whom correspondence should be addressed. F.M.: telephone, (479) 575-4999; fax, (479) 575-4049; e-mail, millett@comp.uark.edu. S.F.-M.: telephone, (517) 353-0199; fax, (517) 353-9334; e-mail, fergus20@pilot.msu.edu.

‡ Michigan State University.

§ University of Arkansas.

|| Current address: Centre for Vascular Research, University of New South Wales, Sydney, NSW 2052, Australia.

[1] Abbreviations: C*c*O, cytochrome *c* oxidase; COV, cytochrome *c* oxidase vesicle; 3CP, 3-carboxyl-2,2,5,5-tetramethyl-1-pyrrolidinyloxy free radical; DEAE, diethylaminoethyl; EPR, electron paramagnetic resonance; LM, lauryl maltoside; PCR, polymerase chain reaction; *Rs*, *Rhodobacter sphaeroides*; RCR, respiratory control ratio; $Ru_2C$, ruthenium dimer; RuC*c*, ruthenium complex-labeled cytochrome *c*; TMPD, *N*,*N*,*N*′,*N*′-tetramethyl-*p*-phenylenediamine.

10.1021/bi050283d CCC: $30.25 
Published on Web 07/14/2005

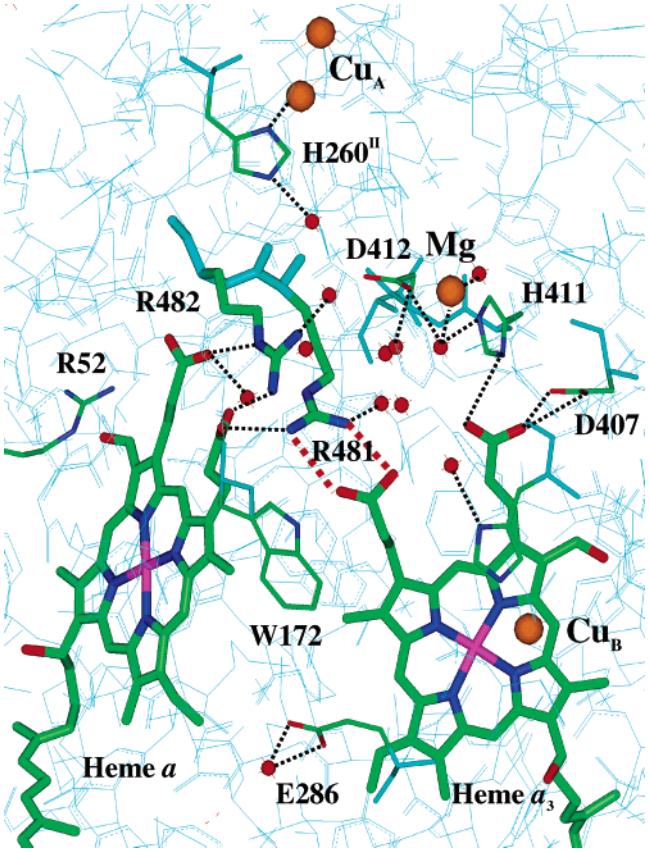


FIGURE 1: Structure of *Rs* C*c*O showing the arginines and their interactions. From the crystal structure (*5*), the figure was made using Insight II. Waters are shown as red spheres. Dotted black lines show hydrogen bonding interactions of ≤3 Å. Dotted red lines show distances of <4 Å that depict electrostatic interactions.

protons from the D path (*18*, *19*). Consistent with this interpretation is the observation of inhibition of wild-type or D132A COVs by externally added zinc. Zinc reduces the activity of the controlled state but not the uncontrolled state (in the absence of $\Delta\mu H^+$) (*20*). This EDTA-reversible inhibition of activity by zinc is observed to correlate with inhibition of the rate of alkalinization of the exterior of the vesicles. The results strongly suggest that backflow of protons is important in the controlled state, to support both the activity of D132A and the activity of the wild type when inhibited by a high $\Delta\mu H^+$.

It has been proposed that protons to be pumped move from residue E286 to the vicinity of the propionates above the hemes (*21*−*24*) before being released to the outside bulk solvent, by an as yet undefined proton exit path (*25*). A possible location for a proton to reside, to accomplish charge neutralization of the incoming electron (*26*), is on the propionates of the hemes [or an associated water (*27*)]. FTIR studies with $^{13}$C-labeled propionates suggest that at least two of the four propionates in the *Paracoccus denitrificans* cytochrome *c* oxidase undergo changes in protonation or environment upon heme reduction (*28*, *29*). In other heme proteins, it has been shown that the protonation state of the propionates of the hemes has a role in controlling the redox potential and cooperativity (*30*, *31*). To examine the possible involvement of the propionates and the region above the hemes in proton movement in C*c*O, mutants have been made of the highly conserved arginine pair (R481 and R482) that interacts with both of the heme propionates (Figure 1) (*22*, *23*, *29*, *32*). Previous reports of mutations of the arginines have pointed to a possible role in proton movement (*23*), while structural analysis and theoretical modeling studies also suggest a facilitated electron transfer pathway between Cu$_A$ and heme *a* in this region (*32*−*34*).

Studies with various R482 mutations, the arginine closely associated with heme *a*, show changes in the electron transfer rates from the electron donor, cytochrome *c*, to Cu$_A$ and between Cu$_A$ and heme *a* (*32*). The conservative mutation of R482 to a lysine was wild-type in its steady-state activity, in both purified and reconstituted forms, but significantly altered in the midpoint potential difference between heme *a* and Cu$_A$ [$\Delta E_m = E_m$(heme *a*) − $E_m$(Cu$_A$), 28 mV in R482K versus 46 mV in the wild type (*32*)]. Alteration of R482 to a hydrophobic residue caused loss of Mg, a non-redox active metal above heme $a_3$, and a disturbed subunit I−subunit II interface. The R482P mutant, which is relatively unstable structurally, shows very slow electron transfer from Cu$_A$ to heme *a*. When both R482 and R481 are mutated to glutamine in the *Escherichia coli bo*$_3$ oxidase, the activity is reduced to less than 50% and there appears to be no proton pumping (*23*).

Arginine 481 is intimately associated with both heme *a* and $a_3$ propionates. From the crystal structure, it appears to be within hydrogen bonding distance (≤3 Å) of the heme *a* D-propionate (Figure 1, black dashed lines) and to have strong electrostatic interactions (<4 Å) with the D-propionate of heme $a_3$ (Figure 1, red dashed lines). Mutation of the conserved R481 in C*c*O to a lysine results in normal activity in the purified enzyme and normal proton pumping efficiency, although the proton pumping is slowed, due to slowed cytochrome *c* oxidation under the reconstituted, pumping conditions (*32*). R481K has no spectrally detectable perturbation of the Cu$_A$ site, even though the peptide backbone of R481 is hydrogen bonded through water to a ligand of Cu$_A$ (H260$^{II}$ in subunit II) (*32*) (Figure 1).

To examine the role of R481 in maintaining the structural and/or electrostatic properties of the propionates, further studies were carried out, including time-resolved measurement of rates of electron transfer from Cu$_A$ to heme *a* in the R481K mutant C*c*O. A double mutant of D132A and R481K was made to test whether mutating the externally located arginine would affect the severely inhibited, internally located D132A mutant, since the latter C*c*O is postulated to rely on protons being supplied from the outside (backflow) for its activity.

## MATERIALS AND METHODS

*Site-Directed Mutagenesis and Protein Purification.* Site-directed mutants were constructed using PCR overlapping extension methods (*35*). For the D132A/R481K double mutation, the pCH81 plasmid, containing the entire Cox I with the D132A mutation (*9*), was used for the second R481K mutation. The primer and construction of R481K were described previously (*32*). The Michigan State University (MSU) Macromolecular Structural Facility, East Lansing, MI, synthesized all of the oligonucleotide primers. The D132A/R481K double mutation, after complete sequencing at the MSU facility, was placed in the histidine tag II construct (*36*) before conjugation into *Rhodobacter sphaeroides*.

Cytochrome *c* oxidase was extracted from *Rs* grown in Sistrom's media as described previously (*37*), and purified on a Ni−NTA affinity column (*38*). Modifications were made to this protocol to maintain binding of the His tag II C*c*O. Ni−NTA (Qiagen) was suspended in high-salt buffer [10 mM Tris-HCl (pH 8.0), 10 mM imidazole, 200 mM KCl, and 0.1% lauryl maltoside (LM)] for the binding procedure. High-salt buffers were used for the Ni−NTA wash and elution of C*c*O. The protein, after Ni−NTA affinity chromatography, was further washed with 10 mM HEPES-KOH (pH 7.4), 0.1% lauryl maltoside, and 40 mM KCl using a Centricon-50 concentrator (Amicon) to remove Ni-bound histidine. Prior to reconstitution into vesicles, a second ion exchange chromatography purification step was used with two DEAE columns in tandem (Tosohaas DEAE-5PW, 10 $\mu$m particle size, 8 mm × 7.5 cm) using a Pharmacia ÃKTA FPLC system as previously described (*36*).

*Reconstitution of Cytochrome c Oxidase.* Cytochrome *c* oxidase vesicles were prepared as described previously (*9*, *37*) by the sonication of 40 mg/mL asolectin (recrystallized soybean phospholipids from Associated Concentrates) in 2% sodium cholate (Anatrace) and 75 mM HEPES-KOH (pH 7.4). The lipids were mixed 1:1 with 4 $\mu$M C*c*O in 75 mM HEPES-KOH (pH 7.4) with 4% cholate to give final concentrations of 2 $\mu$M oxidase, 20 mg/mL asolectin, and 3% sodium cholate. The vesicles were dialyzed against buffer as described previously (*20*). Oxygen consumption assays were performed for the reconstituted enzymes to determine the respiratory control ratio (RCR), which is a test of whether the cytochrome *c* oxidase vesicles (COVs) are able to produce a membrane potential and pH gradient and the enzymes are inserted correctly (*32*, *36*). The RCR for the un-reconstituted enzyme is expected to be 1.

*Measurement of the pH Dependence of CcO Activity.* Steady-state measurements of the activity of cytochrome *c* oxidase were made in a Gilson oxygraph with purified C*c*O, horse heart cytochrome *c*, ascorbate, and TMPD in the appropriate buffer (HEPES-KOH, MES-KOH, or glycylglycine-KOH) at 50 mM with 0.05% LM and KCl added to maintain a constant ionic strength. Cytochrome *c* oxidation measurements with COVs at different pH values were made in an OLIS-rsm stopped-flow apparatus at 0.1−0.2 $\mu$M $aa_3$ in 50 $\mu$M buffer rapidly mixed with prereduced horse heart cytochrome *c* [in 0.5 mM HEPES-KOH (pH 7.4) and 44 mM KCl] diluted into 40 mM buffer at the appropriate pH (MES-KOH, HEPES-KOH, or glycylglycine-KOH) to give a final concentration after stopped-flow mixing of 20 mM buffer with 45 mM $K^+$ and 22 mM sucrose. Measurements were made (1) in the absence of ionophores for the controlled state, (2) with 2 $\mu$M valinomycin to remove the $\Delta\Psi$, and (3) with 2 $\mu$M valinomycin and 5 $\mu$M FCCP as an uncoupler to allow maximal activity. Ionophores were added to the COVs prior to mixing with C*c*. The kinetic traces were fit exponentially, and the $k_{obs}$ ($s^{-1}$) values were converted to molecular activity (catalytic turnover in electrons per second per $aa_3$) by multiplying $k_{obs}$ by [cyt $c^{2+}$] ($\mu$M)/[$aa_3$] ($\mu$M). The RCR was obtained by dividing the uncontrolled rate by the controlled rate.

*Fast Electron Transfer of Oxidized CcO.* Ru-55-C*c* (ruthenium trisbipyridine-labeled horse heart cytochrome *c*) was used to deliver electrons to the oxidized C*c*O using a laser flash (*39*, *40*). The photoexcited state was formed [Ru-(II) to Ru(II*)] which rapidly transferred an electron to heme *c*. At low ionic strengths, 5 mM Tris-HCl (pH 8.0), Ru-55-C*c* forms a 1:1 complex with C*c*O so that rapid electron transfer from heme *c* to $Cu_A$ and heme *a* in C*c*O can be measured spectrophotometrically at 830 and 605 nm, respectively. The reaction of cytochrome *c* was monitored at 550 nm using an extinction coefficient $\Delta\epsilon_{550}$ of 18.5 $mM^{-1}$ $cm^{-1}$. The reaction of $Cu_A$ was monitored at 830 nm using a $\Delta\epsilon_{830}$ of 2.0 $mM^{-1}$ $cm^{-1}$, and the reduction of heme *a* was assessed at 605 nm using a $\Delta\epsilon_{605}$ of 16 $mM^{-1}$ $cm^{-1}$. The reduction of heme *a* was also monitored in some experiments with a high-sensitivity detector with a 600 nm band-pass filter with a band-pass of 10 nm. The effective extinction coefficient for heme *a* in this system was 9.6 $mM^{-1}$ (*41*). Reaction solutions typically contained 3−10 $\mu$M Ru-C*c*, 5−20 $\mu$M C*c*O, 10 mM aniline, and 1 mM 3CP in 5 mM Tris-HCl (pH 8.0) at 22 °C. The aniline and 3CP functioned as sacrificial electron donors to reduce Ru(III) and prevent the back reaction with heme $Fe^{2+}$. The ionic strength was increased, up to 300 mM NaCl, to measure the effect of the mutation on the interaction of Ru-55-C*c* with C*c*O. The transients were fitted to appropriate theoretical equations for Scheme 1 as described by Geren et al. (*39*). Additionally, the pH was altered; pH 6.5 and 8.0 were used, and the effect on the rates was measured.

Scheme 1

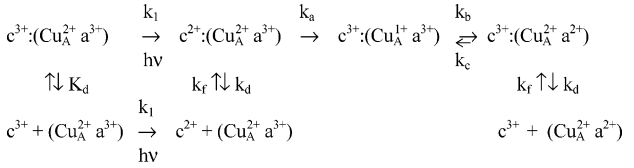


The reduction of C*c*O by the photoexcited ruthenium dimer, $Ru_2C$, was studied to resolve the rapid electron transfer reaction between $Cu_A$ and heme *a*. Reaction mixtures consisted of 12 $\mu$M C*c*O, 25 $\mu$M $Ru_2C$, 10 mM aniline, and 1 mM 3CP in 5 mM Tris-HCl (pH 8.0). The absorbance transient was recorded at 605 nm using a monochromator detector with a time resolution of 20 ns, as described by Zaslavsky et al. (*42*).

*Dithionite Reduction of CcO.* Measurements of the rates of heme *a* and heme $a_3$ reduction of C*c*O with sodium dithionite were performed in a stopped-flow rapid scanning spectrophotometer (OLIS rsm-16) under anaerobic conditions. Sodium dithionite in argon-sparged buffer was rapidly mixed with C*c*O in the same anaerobic buffer to give a final concentration of 15 mM sodium dithionite and 2 $\mu$M wild-type or mutant C*c*O; 1000 scans/s were collected from 390 to 630 nm. At least three data sets were collected and averaged for each measurement. These measurements were then repeated with newly prepared samples. Reduced minus oxidized difference spectra were analyzed using the OLIS Global fitting software provided for identification of the kinetically independent species (*a* and $a_3$). This was compared to the first-order rate constants for single wavelengths at 605 and 428 nm for heme *a* and 434 nm for heme *a* plus $a_3$ to ensure that a true fit was obtained. The measurements were made with two different buffers: (A) 200 mM HEPES-KOH (pH 8.0) and 0.1% LM and (B) 200 mM Bis-Tris-propane (pH 6.5) and 0.1% LM (*43*).

*Other Spectral Assays.* Examination of binding of CO to C*c*O was performed as described previously (*37*) on a Perkin-

Table 1: Cytochrome *c* Reduction Rates of Wild-Type and Mutant C*c*O Reconstituted into COVs[a]

| | activity ($e^- s^{-1} aa_3^{-1}$) | | | | |
|---|---|---|---|---|---|
| COVs | controlled | with valinomycin | uncontrolled | RCR $\Delta\Psi$[b] | RCR[c] |
| wild type | 51 ± 1 | 180 ± 23 | 460 ± 120 | 3.5 | 9 |
| R481K | 13 ± 1 | 45 ± 25 | 210 ± 36 | 3.5 | 16 |
| D132A | 13 ± 3 | 5.6 ± 3 | 14 ± 1 | 0.4 | 1.1 |
| D132A/R481K | 7.9 ± 1.4 | 2.6 ± 5.7 | 3.7 ± 3.5 | 0.3 | 0.5 |

[a] Measurements were made in an OLIS-rsm stopped-flow spectrophotometer at pH 7.4 in the controlled state (with a membrane potential and pH gradient), with valinomycin (no membrane potential), and in the uncontrolled state (with FCCP and valinomycin added) as in Figure 2. Errors shown are the standard deviation from the averaging of at least three data sets. [b] $\Delta\Psi$ respiratory control ratio which is obtained from the rate with valinomycin divided by the controlled rate. [c] Respiratory control ratio which is obtained from the uncontrolled rate divided by the controlled rate.

Elmer Lambda 40P UV−visible spectrophotometer at room temperature.

## RESULTS

*Effect of Reconstitution on Activity.* The maximal steady-state activity of the isolated or reconstituted R481K-mutated oxidase is like that of wild-type C*c*O at 25 °C and pH 6.5 (*32*) but is more inhibited by an increase in pH than that of wild-type C*c*O. When R481K is reconstituted into vesicles (COVs), with a highly buffered interior at pH 7.4 and in the presence of a pH gradient and membrane potential ($\Delta\Psi$), it exhibits low activity relative to that of wild-type C*c*O (Table 1). It is important to note that these measurements are not made with saturating levels of cytochrome *c*, but with limiting amounts under stopped-flow conditions comparable to those used for assessing proton pumping (*32*).

Measurement of the activity versus external pH of wild-type COVs typically shows an apparent p$K_a$ at pH ~7.3 in the controlled state. In the R481K COVs, there is no apparent p$K_a$ within the range of measurement; instead, activity gradually decreases with increasing pH, as in the D path mutant, D132A (Figure 2A). However, in the D132A COVs, the controlled state has an activity (~15 $s^{-1}$) higher than that observed with no membrane potential (~6 $s^{-1}$) (Figure 2B), likely due to the stimulation of proton backflow as indicated by an increased rate of external alkalinization (*18*, *19*). In contrast, the double mutant D132A/R481K is more inhibited in all states (Table 1), supportive of the concept that R481K may further limit proton access.

Under the conditions used to study proton pumping by stopped-flow, when the $\Delta\Psi$ is removed by addition of valinomycin, activity is increased for wild-type C*c*O and R481K over the whole pH range, but R481K was significantly less active than the wild type. This may relate to the observed lower redox potential of heme *a* (Table 2) which becomes more limiting to activity when cytochrome *c* levels are low and $Cu_A$ is not kept fully reduced. At saturating cytochrome *c* concentrations ($V_{max}$), the mutant and wild-type activities are comparable, as in the free enzyme (*32*). In the case of D132A and the double mutant, strong inhibition, rather than stimulation, is observed across the whole pH range when the membrane potential is removed (Figure 2B). This "reverse respiratory control" has been previously observed (*19*). In the case of R481K, a lower than wild-type controlled rate, but a stimulated uncontrolled rate, results in an increase in the respiratory control ratio (RCR). The RCR for R481K is well above that seen for the wild type in stopped-flow measurements of cytochrome *c* oxidation (Table 1 and ref *44*) and more like that obtained with the addition of zinc to the outside of wild-type COVs in the controlled state (*20*). Both D132A and D132A/R481K show inhibition of activity when the membrane potential is removed (by the addition of valinomycin) unlike the wild type and R481K, resulting in a $RCR_{\Delta\Psi}$ of <1 (Table 1). This phenomenon can be explained by the removal of the driving force for proton backflow to support activity.

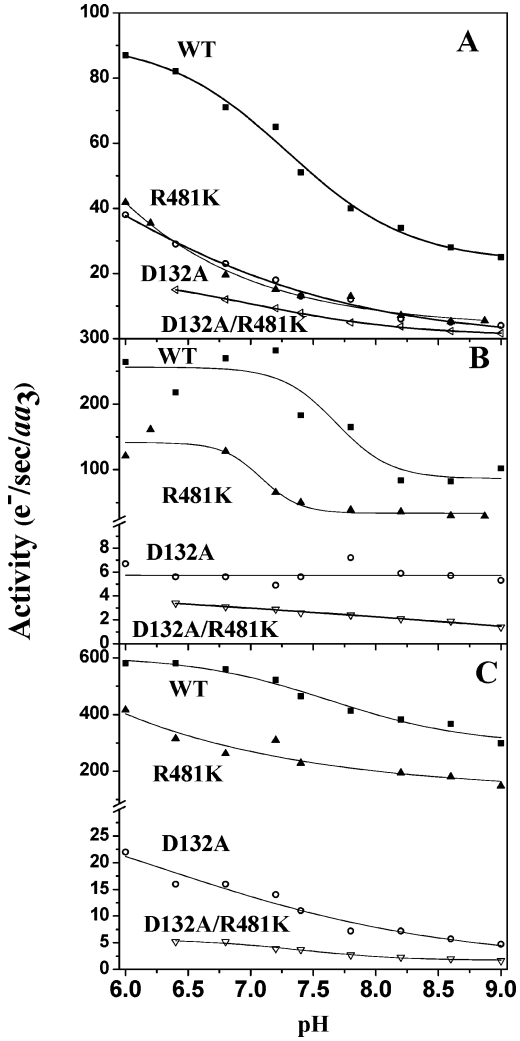


FIGURE 2: Activity of R481K C*c*O, reconstituted into lipid vesicles, inhibited in the presence of a $\Delta\Psi$, in the controlled state, and its activity compared to those of wild-type, D132A, and D132A/R481K COVs (see Materials and Methods) across the pH range from 6.0 to 9.0: (A) controlled-state activity, (B) activity in the absence of a membrane potential after the addition of 1 $\mu$M valinomycin, but with a pH gradient, and (C) uncontrolled activity, with both valinomycin and 5 $\mu$M FCCP.

In the uncontrolled state, when both the membrane potential and pH gradient are removed, the activities of wild-type C*c*O and R481K C*c*O are stimulated (Figure 2C). D132A and the double mutant, D132A/R481K, are slightly stimulated, but these activities remain much lower than that of the wild type, consistent with blockage of backflow and uptake of protons in the double mutant.

Table 2: Electron Transfer Reaction between $Cu_A$ and Heme *a* in C*c*O Mutants[a]

| C*c*O | $K$ ($k_b/k_c$) | $\Delta E_m$ (mV) (heme *a* − $Cu_A$) | $k_a$ ($\times 10^4$ $s^{-1}$) | $k_b$ ($\times 10^4$ $s^{-1}$) | $k_c$ ($\times 10^4$ $s^{-1}$) |
|---|---|---|---|---|---|
| wild type | 5.4 ± 1.0 | 43 ± 5 | 4.0 ± 0.5 | 9.3 ± 1.5 | 1.7 ± 3.0 |
| R481K | 1.4 ± 0.6 | 8 ± 12 | 4.0 ± 0.5 | 5.1 ± 1.0 | 3.7 ± 0.7 |
| D132A | 6.3 ± 1.0 | 47 ± 4 | 3.4 ± 0.5 | – | – |
| D132A/R481K | 1.5 ± 0.6 | 10 ± 12 | 2.5 ± 0.5 | 7.2 ± 1.5 | 4.8 ± 1.0 |

[a] The equilibrium constant ($K = k_b/k_c$) is from the ratios of reduction of $Cu_A$ and heme *a* by Ru-55-C*c*, as described in the legend of Figure 4. The $\Delta E_m$ between heme *a* and $Cu_A$ was calculated from *K*. The rate constant $k_{obs}$ for electron transfer from $Cu_A$ to heme *a* was measured using $Ru_2C$ to photoreduce $Cu_A$, as described in Materials and Methods. The values of $k_b$ and $k_c$ were calculated from $k_{obs}$ and *K* as described in the text.

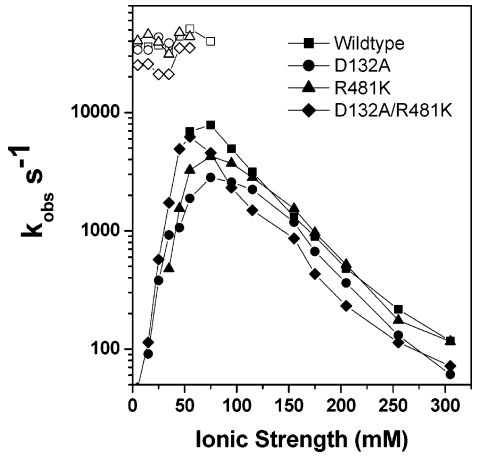


FIGURE 3: Ionic strength dependence of the fast intracomplex phase, $K_a$ (empty symbols), and the slow phase (filled symbols) of the reactions between Ru-55-C*c* and $Cu_A$ in C*c*O mutants. The solutions contained 10 $\mu$M Ru-55-C*c* and 15 $\mu$M C*c*O in 5 mM Tris-HCl (pH 8.0), 0−300 mM NaCl, 10 mM aniline, and 1 mM 3CP.

When the $\Delta\Psi$ is removed, both the wild type and R481K are able to pump protons with a net $H^+/e^-$ stoichiometry of ~1 (*32*), but D132A shows no net proton pumping and has very low activity across the pH range, which correlates with rates of external alkalinization in the controlled state (*18*, *19*) (Figure 2B). The double mutant, D132A/R481K, also shows no net proton pumping and significant but slow activity, correlated with alkalinization in the controlled state (data not shown).

*Fast Electron Transfer Measurements of Oxidized C*c*O.* A horse cytochrome *c* derivative with a ruthenium trisbipyridine complex covalently attached to lysine 55, Ru-55-C*c*, is used as an electron donor for oxidized C*c*O. At low ionic strengths, Ru-55-C*c* forms a 1:1 complex with C*c*O. Photoexcitation of the Ru(II) group to a metal-to-ligand charge transfer state, Ru(II*), results in rapid reduction of heme *c*, followed by intracomplex electron transfer from heme *c* to $Cu_A$ with rate constant $k_a$ (Scheme 1) (*41*). The intracomplex rate constant $k_a$ at low ionic strengths was found to be 4.0 $\times$ $10^4$ $s^{-1}$ for wild-type C*c*O, compared with rates of 4.0 $\times$ $10^4$, 3.4 $\times$ $10^4$, and 2.5 $\times$ $10^4$ $s^{-1}$ for the R481K, D132A, and D132A/R481D mutants, respectively (Table 2 and Figure 3). Following reduction of $Cu_A$, an electron is transferred from $Cu_A$ to heme *a* with a rate constant $k_b$ (Scheme 1). The value of $k_b$ is larger than the value of $k_a$ and so cannot be measured using Ru-55-C*c*; however, this rate constant can be measured using a ruthenium dimer for photoreduction (see below and ref *42*). The kinetics and the $k_a$ values for wild-type C*c*O and the other mutants do not change significantly at an ionic strength of up to 40 mM. At higher ionic strengths, the amplitude of the fast intracomplex phase decreased due to an increased level of dissociation of the 1:1 complex, and

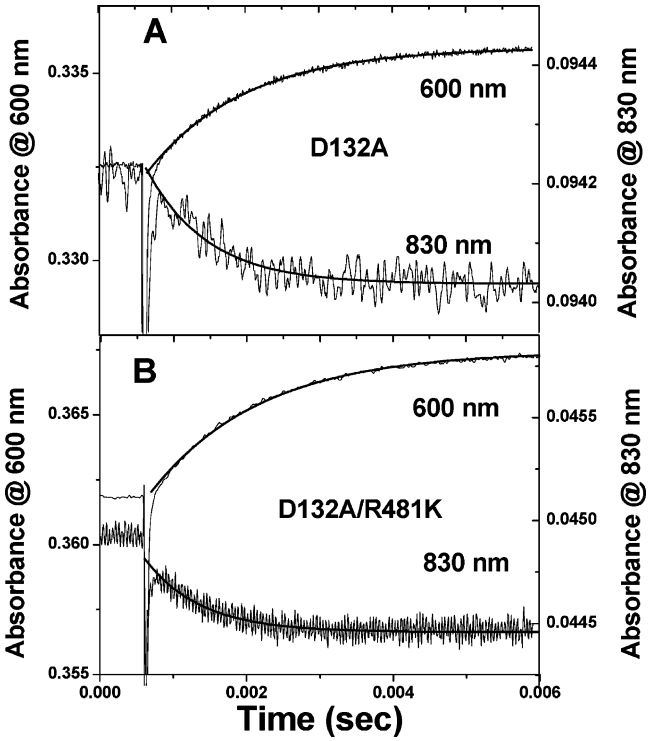


FIGURE 4: Photoinduced electron transfer from Ru-55-C*c* to *Rs* C*c*O mutants. (A) A sample containing 10.5 $\mu$M D132A C*c*O and 12.7 $\mu$M Ru-55-C*c* in 5 mM Tris-HCl (pH 8) with 10 mM aniline, 1 mM 3CP, and 170 mM NaCl was photoexcited with a 200 ns laser flash at 480 nm. The rate constants for reduction of heme *a* and $Cu_A$, measured at 600 and 830 nm, were 880 ± 200 and 1000 ± 200 $s^{-1}$, respectively. (B) The sample contained 13.4 $\mu$M D132A/R481K C*c*O and 9.9 $\mu$M Ru-55-C*c* in 5 mM Tris-HCl (pH 8) with 150 mM NaCl.

a new slow phase appears due to the reaction of Ru-55-C*c* from a solution with C*c*O (Figure 3). The rate constant of the slow bimolecular phase increased to a maximum at an ionic strength of 70 mM, and then decreased with further increases in ionic strength. The slow phase rate constants of the D132A and R481K mutants were nearly the same as that of wild-type C*c*O at all ionic strengths, while the values for the D132A/R481K mutant were somewhat smaller (Figure 3). The slow phase rate constant is controlled by dissociation of the C*c*−C*c*O complex at ionic strengths of up to 70 mM, and by formation of the 1:1 complex at high ionic strengths (*41*). These results indicate that the mutations examined in this study had relatively small effects on the binding affinity with Ru-55-C*c*.

The ratio of reduced heme *a* to $Cu_A$, providing a measure of equilibrium constant *K*, was obtained from the relative amplitudes of the 600 and 830 nm transients after equilibrium was reached, as shown in Figure 4. These experiments were carried out at high ionic strengths, where only the slow

bimolecular phase was present. The value of $K$ ($=k_b/k_c$) was found to be 6.3 ± 1.0 for the D132A mutant (Figure 4A), which corresponds to a difference in midpoint potential between heme *a* and $Cu_A$ [$\Delta E_m = E_m$(heme *a*) − $E_m(Cu_A)$] of 47 ± 4 mV (Table 2). This is the same as previously determined for wild-type C*c*O [$K = 5.4 \pm 1.0$, $\Delta E_m = 43 \pm 5$ mV (*41*)]. However, the values of $K$ for the D132A/R481K and R481K mutants are much lower than that of wild-type C*c*O (Figure 4B and Table 2). The $K$ value for D132A/R481K is 1.5 ± 0.6 (Figure 4), corresponding to a $\Delta E_m$ of 10 ± 12 mV. The values for the R481K mutant are as follows: $K = 1.4 \pm 0.6$ and $\Delta E_m = 8 \pm 12$ mV. This demonstrates that the electron has a stronger tendency to remain on $Cu_A$ in the R481K and D132A/R481K C*c*O mutants, suggesting an alteration in the $\Delta E_m$ of either heme *a* (decreased) or $Cu_A$ (increased). A change in the heme *a* site seems to be most probable, due to a likely change in the proximity of K481 to the propionic acid groups in heme *a* (see S. A. Seibold et al., accompanying paper).

To study the rapid electron transfer between $Cu_A$ and heme *a* ($k_b$), C*c*O was reduced with the photoexcited ruthenium dimer, $Ru_2C$, as described by Zaslavsky et al. (*42*). $Ru_2C$ has a charge of +4 which allows it to bind to the cytochrome *c* binding domain on subunit II near $Cu_A$. The photoexcited state of $Ru_2C$ reduces $Cu_A$ within 1 μs, allowing the electron transfer reaction between $Cu_A$ and heme *a* to be resolved (*42*). The rate constants for wild-type C*c*O were previously determined: $k_b = 9.3 \times 10^4$ s$^{-1}$ and $k_c = 1.7 \times 10^4$ s$^{-1}$ from a $k_{obs}$ of $11 \times 10^4$ s$^{-1}$ (*42*). For the R481K mutant C*c*O, heme *a* is reduced with a rate constant $k_{obs}$ of $8.8 \times 10^4$ s$^{-1}$ [under reaction conditions of 25 μM $Ru_2C$ with 12 μM R481K C*c*O in 5 mM Tris-HCl (pH 8.0) containing 10 mM aniline and 1 mM 3CP]. Using the relations $K = k_b/k_c = 1.4$ and $k_{obs} = k_b + k_c$, the values of $k_b$ and $k_c$ are calculated: $k_b = 5.1 \times 10^4$ s$^{-1}$ and $k_c = 3.7 \times 10^4$ s$^{-1}$. For the D132A/R481K double mutant, heme *a* is reduced with a rate constant $k_{obs}$ of $12 \times 10^4$, so using a $K$ of 1.5 the rate constants are calculated to be $7.2 \times 10^4$ s$^{-1}$ ($k_b$) and $4.8 \times 10^4$ s$^{-1}$ ($k_c$).

*Reduction Kinetics of Heme a and $a_3$.* C*c*O has a characteristic absorption spectrum in the Soret region with a broad peak when oxidized at 420 and 446 nm when fully reduced. These Soret peaks contain contributions from both the low-spin six-coordinate heme *a*, and heme $a_3$, the active site where oxygen binds (*45*). Additionally, there are absorption peaks at higher wavelengths, particularly a peak at 606 nm where ~80% of the absorption is contributed by reduced heme *a* (*45*). To observe the effects of R481K on the kinetic behavior of individual hemes, measurements were made using sodium dithionite as a reducing agent under anaerobic conditions with rapid mixing in a stopped-flow rapid scanning spectrophotometer.

The spectral scans of wild-type (Figure 5, left panel) and R481K C*c*O (Figure 5, middle panel) are shown for 2.5 s of the reaction with sodium dithionite. The reduction of heme *a* is complete for both the wild type and R481K within this time, as seen by the peak absorbance at 606 nm. However, the Soret band is still split after 2.5 s, with peaks at 420 and 442 nm, because heme $a_3$ is still not fully reduced: R481K C*c*O exhibits a lower absorbance at 442 nm and a higher absorbance at 420 nm, while wild-type C*c*O shows the opposite. Heme $a_3$ in R481K remains more oxidized than heme $a_3$ of wild-type C*c*O. This difference in the rate of reduction of heme $a_3$ is quantified by global fitting of the spectra to obtain the rates of heme *a* and heme $a_3$ reduction, which are monophasic and complete in all cases (Figure 5, right panel, and Table 3). Both heme *a* and heme $a_3$ were more quickly reduced at low pH, 3.5-fold for heme *a* but <2-fold for heme $a_3$, reflecting the complex dependence on the level of heme *a* reduction. In the R481K mutant, heme $a_3$ reduction is considerably slowed at both pH 6.5 and 8 compared to that of the wild type, while the D path mutant, D132A, shows wild-type rates of both heme *a* and heme $a_3$ at both pH values (Table 3) (as seen in ref *16* but compare with ref *46*). The D132A/R481K double mutant has lowered rates of reduction for both heme *a* and heme $a_3$ at both pH values.

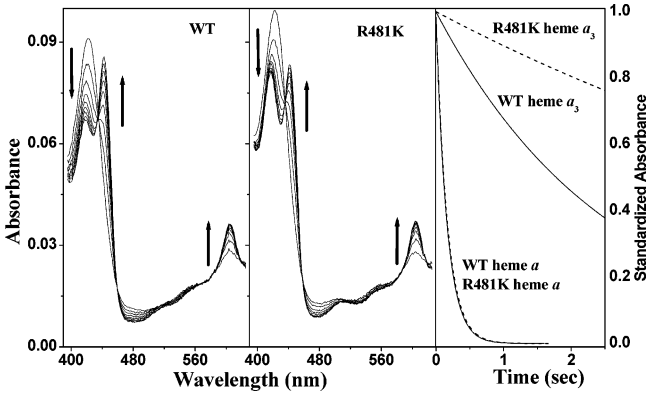


FIGURE 5: Heme $a_3$ of R481K C*c*O is slowly reduced with sodium dithionite. Panels on the left show the spectral scans from OLIS-rsm stopped-flow measurements, up to 2.5 s in steps of 310 ms, after mixing 2 μM wild-type or R481K C*c*O with 15 mM sodium dithionite at pH 6.5 as described in Materials and Methods. Arrows depict the direction of the changes associated with reduction. The panel on the right shows the kinetic traces of heme *a* and heme $a_3$ reduction for the wild type (solid line) and R481K (dashed line) from global fitting of the spectral scans.

Table 3: Reduction Rates of Wild-Type and R481K C*c*O from Global Analysis[a]

| | rate of reduction, $k_{obs}$ (s$^{-1}$) | | | |
|---|---|---|---|---|
| | pH 6.5 | | pH 8 | |
| C*c*O | heme *a* | heme $a_3$ | heme *a* | heme $a_3$ |
| wild type | 6.42 ± 0.78 | 0.49 ± 0.09 | 2.09 ± 0.54 | 0.22 ± 0.04 |
| R481K | 6.10 ± 0.30 | 0.11 ± 0.04 | 1.52 ± 0.20 | 0.05 ± 0.01 |
| D132A | 6.19 ± 0.79 | 0.48 ± 0.07 | 2.24 ± 0.16 | 0.23 ± 0.06 |
| D132A/R481K | 2.51 ± 0.18 | 0.18 ± 0.00 | 1.34 ± 0.02 | 0.09 ± 0.01 |

[a] Sodium dithionite was rapidly mixed with wild-type or R481K C*c*O in a stopped-flow rapid scanning spectrophotometer (OLIS rsm-16) (see Figure 5). Global fitting of the resulting spectral scans from the averaging of at least two separate measurements of three data sets gave kinetic rates ($k_{obs}$, s$^{-1}$) of reduction for each of the hemes. Standard deviations given are from the averaging of data sets.

## DISCUSSION

*Minor Structural Effects of the R481K Mutation.* To interpret the results of these studies, it is important to note that the conservative change of R481 to a lysine has a very minor effect on the overall structure as indicated by native visible spectra for the hemes. The $Cu_A$ site was also not disturbed, as determined by visible and EPR spectroscopy (*32*). The non-redox active Mg or Mn above the hemes is

minimally altered as seen in the hyperfine splittings of the EPR spectrum with possibly slight changes in the orientation of the bound ligands (*32*). There is a shift in the EPR spectrum of heme *a* from $g = 2.83$ to $g = 2.85$ in R481K as well as several R482 mutants. Curiously, despite no change in the visible spectrum of the oxidized or reduced R481K C*c*O, when CO binds to heme $a_3$ of R481K a Soret peak more broadened than that for the wild-type CO-bound form was observed, with a 4 nm shift to a longer wavelength. Besides these minor effects, the R481K mutation is not structurally disruptive.

*Arginines 481 and 482 Are Important for Maintaining the Redox Potential of Heme a.* The control of redox potential changes in heme proteins is an important issue, particularly in C*c*O where the movement of protons is tightly coupled to electron movement (*43*, *46*). Arginine 482 was shown to be important for maintaining the $\Delta E_m$ of heme *a* in C*c*O, with various mutations lowering the $\Delta E_m$ between $Cu_A$ and heme *a* to as low as 18 mV as compared to a value of 46 mV for the wild type.

The fast electron transfer measurements in this study show that the $k_a$ rate constants for intracomplex electron transfer from Ru-55-C*c* to $Cu_A$ are $4.0 \times 10^4$, $3.4 \times 10^4$, and $2.5 \times 10^4$ $s^{-1}$ for the R481K, D132A, and D132A/R481K mutants, respectively, compared with a value of $4.0 \times 10^4$ $s^{-1}$ for wild-type C*c*O (Table 2 and Figure 3). The $k_b$ rate constant for electron transfer from $Cu_A$ to heme *a* is $9.3 \times 10^4$ $s^{-1}$ for wild-type C*c*O, compared with a value of $5.1 \times 10^4$ $s^{-1}$ for the R481K mutant and a value of $7.2 \times 10^4$ $s^{-1}$ for the D132A/R481K mutant (Table 2). In the case of the R481K mutant, the rates of electron transfer from cyt *c* to $Cu_A$ ($k_a$) are similar to those of wild-type C*c*O and D132A C*c*O, while the rates between $Cu_A$ and heme *a* are altered in the R481K mutant and the double mutant. The intrinsic electron transfer rates are all sufficiently fast that they are not rate-limiting in steady-state measurements of activity under conditions of excess reduced cytochrome *c* (*32*). However, the lower equilibrium constant between $Cu_A$ and heme *a* in R481K and the double mutant, reflected in single-electron input experiments, shows that the electron has a tendency to remain on $Cu_A$ in the mutant compared to that in the wild type. This change is calculated to be a $\Delta E_m$ of $Cu_A$ minus heme *a* of approximately 40 mV. It is interpreted to be due to a less positive midpoint potential of heme *a*, since $Cu_A$ is less intimately associated with the mutation and shows no change in spectral characteristics or in the rate of electron transfer from C*c* to $Cu_A$. This change in $\Delta E_m$ could be due to blockage of proton access from the outside via a backflow path that is needed for protonation of a group (or a bound water molecule) involved in determining the redox potential of heme *a* (*47*). Alternatively, the structural and charge distribution changes close to the heme propionates caused by the R481K mutation could be the cause of the potential shift. In a molecular dynamics simulation (S. A. Seibold et al., accompanying paper), the lysine substituted at position 481 is observed to interact more closely with the heme $a_3$ propionates than the native C*c*O arginine, which could affect the protonation state of the propionates and/or the $\Delta E_m$ of the heme.

*Heme $a_3$ Reduction Is Slowed in R481K CcO.* Using sodium dithionite under anaerobic conditions, heme $a_3$ reduction is slowed in R481K C*c*O 4-fold relative to that in wild-type C*c*O at both pH 6.5 and 8.0, but the mutation has no effect on the apparent heme *a* reduction rate, despite the fact that the $\Delta E_m$ of heme *a* is lowered by $\cong$40 mV. The mutant behaves as if it were caught in a "resting" state similar to that seen in bovine C*c*O, in which the electron transfer between heme *a* and heme $a_3$ is observed to be inhibited (*46*, *48*). In the bovine C*c*O, there is evidence that in the fully oxidized (resting) enzyme the midpoint redox potential of heme $a_3$ is low and proton uptake is required to increase the $\Delta E_m$ (*46*, *49*). It is possible that the R481K mutation affects an internal proton movement or binding site occupancy that is important for controlling electron transfer from heme *a* to heme $a_3$ and that at high pH this proton movement or occupancy becomes even less favorable. One such proton binding site is the D-propionate of heme $a_3$, as suggested by Brändén et al. (accompanying paper) to account for the p$K_a$ change for the F $\rightarrow$ O change in R481K. The molecular dynamics studies of Seibold et al. (accompanying paper) also show major changes in structure close to this propionate. Another protonation site associated with heme *a* (*22*) may also be changed in its proton affinity, making protons less available for supporting electron transfer to heme $a_3$, and causing the observed lower redox potential of heme *a* reported in this paper and by Brändén et al. (accompanying paper). In the reduced enzyme used in the rapid kinetic measurements, protons may be already loaded so that electron transfer is not necessarily rate limited.

In contrast, D132A C*c*O, which is known to be inhibited in proton uptake into the D channel, is like the wild type in its reduction with sodium dithionite for both hemes, in electron transfer from $Cu_A$ to heme *a*, and in the relative redox potentials of heme *a* and $Cu_A$ in the oxidized enzyme (but see ref *50*), consistent with no disturbance in the structure of the region above the hemes.

*Mutant R481K CcO Is Inhibited in the Presence of a Membrane Potential.* The measurement of activity in COVs with a stopped-flow spectrophotometer allows rapid mixing of the COVs at pH 7.4 with almost no external buffering (50 $\mu$M) with cytochrome *c* in high-concentration buffers at varying pH values. This technique allows the rapid introduction of a different pH on the outside of the COVs. Under the conditions that were used, there is only enough prereduced cytochrome *c* to give 10 turnovers on average. This means that substrate cytochrome *c* is not saturating as under steady-state conditions. These stopped-flow conditions are observed to increase the stimulatory effect of removal of the membrane potential by the addition of valinomycin, while in steady-state measurements, much less stimulation is observed. This observation can be explained by the fact that electron transfer from $Cu_A$ to heme *a* is working against the membrane potential. When this step is limiting, due to low levels of reduction of $Cu_A$, the overall C*c*O rate becomes very sensitive to the membrane potential (*51*). In the steady state, when cytochrome *c* is saturating, the results with R481K show that the heme *a* midpoint potential can be substantially altered without causing a change in the steady-state activity of the enzyme. However, in the stopped-flow experiments, under the constraints of a membrane potential (controlled conditions), the activity of R481K C*c*O is considerably slower than that of wild-type C*c*O, causing an increased RCR. This inhibition is likely due to the more negative heme *a* potential adding to the more negative

internal membrane potential that inhibits the $Cu_A$ to heme *a* equilibrium electron transfer.

In the D132A mutant, proton uptake from the inside becomes very slow but appears to be driven from the outside in the reverse direction by a membrane potential. Interestingly, this mutant does not affect electron transfer to heme *a*, or the heme *a* midpoint potential. These data suggest that a proton may be supplied from the outside in D132A for slow heme *a* to $a_3$ reduction in the controlled state, but the kinetics of access of that proton is inhibited by the R481K mutation, causing the further inhibition of the R481K/D132A double mutant. When C*c*O is deprived of D path protons (D132A), suicide inactivation is induced, particularly when subunit III is removed. It is interesting that the D132A/R481K double mutant suicide inactivates very rapidly even in the presence of subunit III, supporting the idea that R481K restricts proton access (*52*).

*Role of R481 in CcO.* The proposal that there is a site(s) for a proton(s) in a region above the hemes involved in the reduction of heme *a* to $a_3$ led to the idea that arginine 481 and/or the propionates are candidates for this site (*22*, *23*). The above results are consistent with a direct role of R481 in controlling protonation during pumping, through its influence on the protonation state of the propionates. Indeed, the role of arginine 82 in bacteriorhodopsin could serve as a model for R481 in C*c*O. Both arginine and lysine could perform a similar function [albeit with different facility (*53*)] of moving in response to a change in the protonation state (e.g., the heme $a_3$ D-propionate) and influencing the protonation at a nearby site (e.g., the heme *a* D-propionate). This is consistent with the MD calculations in wild-type and mutant C*c*O (S. A. Seibold et al., accompanying paper). The propionates themselves, therefore, remain strong candidates for sites of protonation.

Electrostatic effects from the alteration of an arginine to a lysine could be the source of the altered $\Delta E_m$ of the hemes and of altered p*K* values of one or more propionates. These effects can provide an explanation of the observed activity changes reported in this paper. However, the molecular dynamic simulations reported in the accompanying paper (S. A. Seibold et al.) suggest that even the very conservative change of R481 to lysine causes significant repercussions in terms of loop movement and amino acid rotamer positions which affect water chain formation. The idea of an arginine−propionate interaction being involved in the control of water was inferred in cytochrome P450 heme enzymes (*54*) where an arginine that interacts with a heme propionate is proposed to act as a mediator in the formation of water chains. Further computational and kinetic studies for examining the effect of R481K on the structure and function of C*c*O are reported in accompanying papers (S. A. Seibold et al. and G. Brändén et al.), while crystallographic and other structural studies are being pursued.

## ACKNOWLEDGMENT

We thank Dr. Denis Proshlyakov for providing the CO for the binding studies and Kori Henry for help with construction of the double mutant, R481K/D132A.

## REFERENCES

1. Ferguson-Miller, S., and Babcock, G. (1996) Heme/copper terminal oxidases, *Chem. Rev. 96*, 2889−2907.
2. Iwata, S., Ostermeier, C., Ludwig, B., and Michel, H. (1995) Structure at 2.8 Å resolution of cytochrome *c* oxidase from *Paracoccus denitrificans*, *Nature 376*, 660−669.
3. Tsukihara, T., Aoyama, H., Yamashita, E., Tomizaki, T., Yamaguchi, H., Shinzawa-Itoh, K., Nakashima, R., Yaono, R., and Yoshikawa, S. (1996) The whole structure of the 13-subunit oxidized cytochrome *c* oxidase at 2.8 Å, *Science 272*, 1136−1144.
4. Ostermeier, C., Harrenga, A., Ermler, U., and Michel, H. (1997) Structure at 2.7 Å resolution of the *Paracoccus denitrificans* two-subunit cytochrome *c* oxidase complexed with an antibody Fv fragment, *Proc. Natl. Acad. Sci. U.S.A. 94*, 10547−10553.
5. Svensson-Ek, M., Abramson, J., Larsson, G., Tornoth, S., Brzezinski, P., and Iwata, S. (2002) The X-ray crystal structures of wild-type and EQ(I-286) mutant cytochrome *c* oxidases from *Rhodobacter sphaeroides*, *J. Mol. Biol. 321*, 329−339.
6. Hosler, J. P., Ferguson-Miller, S., Calhoun, M. W., Thomas, J. W., Hill, J., Lemieux, L., Ma, J., Georgiou, C., Fetter, J., Shapleigh, J. P., Tecklenburg, M. M. J., Babcock, G. T., and Gennis, R. B. (1993) Insight into the active-site structure and function of cytochrome *c* oxidase by analysis of site-directed mutants of bacterial cytochrome $aa_3$ and cytochrome *bo*, *J. Bioenerg. Biomembr. 25*, 121−136.
7. Thomas, J. W., Lemieux, L. J., Alben, J. O., and Gennis, R. B. (1993) Site-directed mutagenesis of highly conserved residues in helix VIII of subunit I of the cytochrome *bo* ubiquinol oxidase from *Escherichia coli*: An amphipathic transmembrane helix that may be important in conveying protons to the binuclear center, *Biochemistry 32*, 11173−11180.
8. Garcia-Horsman, J. A., Puustinen, A., Gennis, R. B., and Wikstrom, M. (1995) Proton transfer in cytochrome $bo_3$ ubiquinol oxidase of *Escherichia coli*: Second-site mutations in subunit I that restore proton pumping in the mutant Asp135→Asn, *Biochemistry 34*, 4428−4433.
9. Fetter, J. R., Qian, J., Shapleigh, J., Thomas, J. W., García-Horsman, J. A., Schmidt, E., Hosler, J., Babcock, G. T., Gennis, R. B., and Ferguson-Miller, S. (1995) Possible proton relay pathways in cytochrome *c* oxidase, *Proc. Natl. Acad. Sci. U.S.A. 92*, 1604−1608.
10. Hosler, J. P., Shapleigh, J. P., Mitchell, D. M., Kim, Y., Pressler, M., Georgiou, C., Babcock, G. T., Alben, J. O., Ferguson-Miller, S., and Gennis, R. B. (1996) Polar residues in helix VIII of subunit I of cytochrome *c* oxidase influence the activity and the structure of the active site, *Biochemistry 35*, 10776−10783.
11. Tsukihara, T., Aoyama, H., Yamashita, E., Tomizaki, T., Yamaguchi, H., Shinzawa-itoh, K., Nakashima, R., Yaono, R., and Yoshikawa, S. (1995) Structure of metal sites of oxidized bovine heart cytochrome *c* oxidase at 2.8 Å, *Science 269*, 1069−1074.
12. Yoshikawa, S., Shinzawa-Itoh, K., and Tsukihara, T. (2000) X-ray structure and the reaction mechanism of bovine heart cytochrome *c* oxidase, *J. Inorg. Biochem. 82*, 1−7.
13. Tsukihara, T., Shimokata, K., Katayama, Y., Shimada, H., Muramoto, K., Aoyama, H., Mochizuki, M., Shinzawa-Itoh, K., Yamashita, E., Yao, M., Ishimura, Y., and Yoshikawa, S. (2003) The low-spin heme of cytochrome *c* oxidase as the driving element of the proton pumping process, *Proc. Natl. Acad. Sci. U.S.A. 100*, 15304−15309.
14. Lee, H.-M., Das, T., Rousseau, D., Mills, D., Ferguson-Miller, S., and Gennis, R. (2000) Mutations in the putative H-channel in the cytochrome *c* oxidase from *Rhodobacter sphaeroides* show that this channel is not important for proton conduction but reveal modulation of the properties of heme *a*, *Biochemistry 39*, 2989−2996.
15. Junemann, S., Meunier, B., Gennis, R. B., and Rich, P. (1997) Effects of mutation of the conserved lysine-362 in cytochrome *c* oxidase from *Rhodobacter sphaeroides*, *Biochemistry 36*, 14456−14464.
16. Vygodina, T. V., Pecoraro, C., Mitchell, D., Gennis, R., and Konstantinov, A. A. (1998) Mechanism of inhibition of electron transfer by amino acid replacement K362M in a proton channel of *Rhodobacter sphaeroides* cytochrome *c* oxidase, *Biochemistry 37*, 3053−3061.
17. Zaslavsky, D., and Gennis, R. (1998) Substitution of lysine-362 in a putative proton-conducting channel in the cytochrome *c* oxidase from *Rhodobacter sphaeroides* blocks turnover with $O_2$ but not with $H_2O_2$, *Biochemistry 37*, 3062−3067.
18. Zhen, Y., Mills, D., Hoganson, C. W., Lucas, R. L., Shi, W., Babcock, G., and Ferguson-Miller, S. (1999) in *Frontiers of Cellular Bioenergetics: Molecular Biology, Biochemistry and*

*Physiopathology* (Papa, S., Guerrieri, F., and Tager, J. M., Eds.) pp 157−178, Kluwer Academic/Plenum Press, New York.
19. Fetter, J. R., Sharpe, M., Qian, J., Mills, D., Ferguson-Miller, S., and Nicholls, P. (1996) Fatty acids stimulate activity and restore respiratory control in a proton channel mutant of cytochrome *c* oxidase, *FEBS Lett. 393*, 155−160.
20. Mills, D. A., Schmidt, B., Hiser, C., Westley, E., and Ferguson-Miller, S. (2002) Membrane potential-controlled inhibition of cytochrome *c* oxidase by zinc, *J. Biol. Chem. 277*, 14894−14901.
21. Hofacker, I., and Schulten, K. (1998) Oxygen and proton pathways in cytochrome *c* oxidase, *Proteins 30*, 100−107.
22. Michel, H. (1999) Cytochrome *c* oxidase: Catalytic cycle and mechanisms of proton pumping-A discussion, *Biochemistry 38*, 15129−15140.
23. Puustinen, A., and Wikstrom, M. (1999) Proton exit from the heme-copper oxidase of *Escherichia coli*, *Proc. Natl. Acad. Sci. U.S.A. 96*, 35−37.
24. Wikström, M., Verkhovsky, M. I., and Hummer, G. (2003) Water-gated mechanism of proton translocation by cytochrome *c* oxidase, *Biochim. Biophys. Acta 1604*, 61−65.
25. Mills, D. A., Florens, L., Hiser, C., Qian, J., and Ferguson-Miller, S. (2000) Where is "outside" in cytochrome *c* oxidase and how and when do protons get there? *Biochim. Biophys. Acta 1458*, 180−187.
26. Rich, P., Meunier, B., Mitchell, R., and Moody, R. (1996) Coupling of charge and proton movement in cytochrome *c* oxidase, *Biochim. Biophys. Acta 1275*, 91−95.
27. Sharpe, M. A., Qin, L., and Ferguson-Miller, S. (2005) in *Biophysical and Structural Aspects of Bioenergetics* (Wikstrom, M. K. F., Ed.) Royal Society of Biochemistry Books, London.
28. Behr, J., Hellwig, P., Mantele, W., and Michel, H. (1998) Redox dependent changes at the heme propionates in cytochrome *c* oxidase from *Paracoccus denitrificans*: Direct evidence from FTIR difference spectroscopy in combination with heme propionate $^{13}C$ labeling, *Biochemistry 37*, 7400−7406.
29. Behr, J., Michel, H., Mantele, W., and Hellwig, P. (2000) Functional properties of the heme propionates in cytochrome *c* oxidase from *Paracoccus denitrificans*. Evidence from FTIR difference spectroscopy and site-directed mutagenesis, *Biochemistry 39*, 1356−1363.
30. Louro, R. O., Catarino, T., LeGall, J., Turner, D. L., and Xavier, A. V. (2001) Cooperativity between electrons and proton in monomeric cytochrome $c_3$: The importance of mechano-chemical coupling for energy transduction, *ChemBioChem 2*, 831−837.
31. Mills, D. A., and Ferguson-Miller, S. (2003) Understanding the mechanism of proton movement linked to oxygen reduction in cytochrome *c* oxidase: Lessons from other proteins, *FEBS Lett. 545*, 47−51.
32. Qian, J., Mills, D. A., Geren, L., Wang, K., Hoganson, C. W., Schmidt, B., Hiser, C., Babcock, G. T., Durham, B., Millett, F., and Ferguson-Miller, S. (2004) Role of the conserved arginine pair in proton and electron transfer in cytochrome *c* oxidase, *Biochemistry 43*, 5748−5756.
33. Onuchic, J. N., Beratan, D. N., Winkler, J. R., and Gray, H. B. (1992) Pathway analysis of protein electron-transfer reactions, *Annu. Rev. Biophys. Biomol. Struct. 21*, 349−377.
34. Ramirez, B. E., Malmstrom, B. G., Winkler, J. R., and Gray, H. B. (1995) The currents of life: The terminal electron-transfer complex of respiration, *Proc. Natl. Acad. Sci. U.S.A. 92*, 11949−11951.
35. Horton, R. M., Hunt, H. D., Ho, S. N., Pullen, J. K., and Pease, L. R. (1989) Engineering hybrid genes without the use of restriction enzymes: Gene splicing by overlap extension, *Gene 77*, 61−68.
36. Hiser, C., Mills, D. A., Schall, M., and Ferguson-Miller, S. (2001) C-Terminal truncation and histidine-tagging of cytochrome *c* oxidase subunit II reveals the native processing site, shows involvement of the C-terminus in cytochrome *c* binding, and improves the assay for proton pumping, *Biochemistry 40*, 1606−1615.
37. Hosler, J. P., Fetter, J., Tecklenburg, M. M. J., Espe, M., Lerma, C., and Ferguson-Miller, S. (1992) Cytochrome $aa_3$ of *Rhodobacter sphaeroides* as a model for mitochondrial cytochrome *c* oxidase, *J. Biol. Chem. 267*, 24264−24272.
38. Zhen, Y., Qian, J., Follmann, K., Hosler, J., Hayward, T., Nilsson, T., and Ferguson-Miller, S. (1998) Overexpression and purification of cytochrome *c* oxidase from *Rhodobacter sphaeroides*, *Protein Expression Purif. 13*, 326−336.
39. Geren, L. M., Beasley, J. R., Fine, B. R., Saunders, A. J., Hibdon, S., Pielak, G. J., Durham, B., and Millett, F. (1995) Design of a ruthenium-cytochrome *c* derivative to measure electron transfer to the initial acceptor in cytochrome *c* oxidase, *J. Biol. Chem. 270*, 2466−2662.
40. Wang, K., Mei, H., Geren, L., Miller, M. A., Saunders, A., Wang, X., Waldner, J. L., Pielak, G. J., Durham, B., and Millett, F. (1996) Design of a ruthenium-cytochrome *c* derivative to measure electron transfer to the radical cation and oxyferryl heme in cytochrome *c* peroxidase, *Biochemistry 35*, 15107−15119.
41. Wang, K., Zhen, Y., Sadoski, R., Grinnell, S., Geren, L., Ferguson-Miller, S., Durham, B., and Millett, F. (1999) Definition of interaction domain for the reaction of cytochrome *c* with cytochrome *c* oxidase: II. Rapid kinetics analysis of electron transfer from cytochrome *c* to *Rhodobacter sphaeroides* cytochrome oxidase surface mutants, *J. Biol. Chem. 274*, 38042−38050.
42. Zaslavsky, D., Sadoski, R. C., Wang, K., Durham, B., Gennis, R. B., and Millett, F. (1998) Single electron reduction of cytochrome *c* oxidase compound F: Resolution of partial steps by transient spectroscopy, *Biochemistry 37*, 14910−14916.
43. Zhen, Y., Schmidt, B., Kang, U. G., Antholine, W., and Ferguson-Miller, S. (2002) Mutants of the $Cu_A$ site in cytochrome *c* oxidase of *Rhodobacter sphaeroides*: I. Spectral and functional properties, *Biochemistry 41*, 2288−2297.
44. Mills, D. A., and Ferguson-Miller, S. (2002) Influence of structure, pH and membrane potential on proton movement in cytochrome *c* oxidase, *Biochim. Biophys. Acta 1555*, 96−100.
45. Vanneste, W. H. (1966) The stoichiometry and absorption spectra of components *a* and $a_3$ in cytochrome *c* oxidase, *Biochemistry 5*, 838−848.
46. Verkhovsky, M. I., Morgan, J. E., and Wikstrom, M. (1995) Control of electron delivery to the oxygen reduction site of cytochrome *c* oxidase: A role for protons, *Biochemistry 34*, 7483−7491.
47. Forte, E., Scandurra, F., Richter, O.-M. H., D'Itri, E., Sarti, P., Brunori, M., Ludwig, B., and Giuffre, A. (2004) Proton uptake upon anaerobic reduction of *Paracoccus denitrificans* cytochrome *c* oxidase: A kinetic investigation of the K354M and D124N mutants, *Biochemistry 43*, 2957−2963.
48. Brunori, M., Giuffre, A., D'Itri, E., and Sarti, P. (1997) Internal electron transfer in Cu-heme oxidases. Thermodynamic or kinetic control? *J. Biol. Chem. 272*, 19870−19874.
49. Gregory, L., and Ferguson-Miller, S. (1989) Independent control of respiration in cytochrome *c* oxidase vesicles by pH and electrical gradients, *Biochemistry 28*, 2655−2662.
50. Ruitenberg, M., Kaant, A., Bamberg, E., Fendler, K., and Michel, H. (2002) Reduction of cytochrome *c* oxidase by a second electron leads to proton translocation, *Nature 417*, 99−102.
51. Brunori, M., Sarti, P., Colosimo, A., Antonini, G., Malatesta, F., Jones, M., and Wilson, M. (1985) Mechanism of control of cytochrome *c* oxidase activity by the electrochemical-proton gradient, *EMBO J. 4*, 2365−2368.
52. Mills, D. A., and Hosler, J. P. (2005) Slow proton transfer through the pathways for pumped protons in cytochrome *c* oxidase induces suicide inactivation of the enzyme, *Biochemistry 44*, 4656−4666.
53. Hatanaka, M., Sasaki, J., Kandori, H., Ebrey, T., Needleman, R., Lanyi, J. K., and Maeda, A. (1996) Effects of arginine-82 on the interactions of internal water molecules in bacteriorhodopsin, *Biochemistry 35*, 6308−6212.
54. Oprea, T. I., Hummer, G., and Garcia, A. E. (1997) Identification of a functional water channel in cytochrome P450 enzymes, *Proc. Natl. Acad. Sci. U.S.A. 94*, 2133−2138.

BI050283D